Seismic Performance of Lightly Reinforced and Unconfined C-shaped Walls

Ryan D. Hoult[1,2], Helen M. Goldsworthy[1,2], Elisa Lumantarna[1,2]

[1]Department of Infrastructure Engineering, University of Melbourne

[2]Bushfire and Natural Hazard Cooperative Research Centre, Melbourne, Australia

Email: ryan.hoult@unimelb.edu.au

ABSTRACT:

Poor seismic performance has been associated with lightly reinforced and unconfined non-rectangular reinforced concrete (RC) walls in recent earthquake events. The non-rectangular C-shaped RC wall is a popular construction choice for providing lateral stiffness to the building while also enclosing a service core, lifts, stairs or toilets. Given that the current provisions of AS 3600:2009 for the design of RC walls require very little (if any) confinement and allow low amounts of distributed longitudinal reinforcement to be used, an investigation is warranted focusing on the seismic performance of such structural elements. This paper presents an overview of some of the research results from an investigation focusing on the seismic performance of RC C-shaped walls with a range of different parameters that would be commonly found in low-to-moderate seismic regions. An extensive number of finite element modelling analyses were undertaken using VecTor3. The equivalent plastic hinge length results from the analyses are discussed and some recommendations for boundary elements of walls are proposed for the next revision of the AS 3600.

Keywords: U-shaped, concrete, shear walls, cores, low-to-moderate, earthquake

1. Introduction

In regions of low-to-moderate seismicity, such as Australia, the majority of the RC walls are lightly reinforced (Hoult *et al.*, 2017; Wibowo *et al.*, 2013; Wilson *et al.*, 2015). Past and recent research conducted on the seismic performance of lightly reinforced concrete walls has typically focused on rectangular sections (Altheeb, 2016; Cardenas & Magura, 1972; Lu *et al.*, 2016; Oesterle *et al.*, 1976; Puranam & Pujol, 2017). However, RC walls (or cores) are often non-rectangular due to structural and architectural requirements (Belletti *et al.*, 2013; Smyrou *et al.*, 2013). For example, a C-shaped wall is a popular construction choice as it can enclose elevators or stairs (Beyer *et al.*, 2008a). The behaviour of C-shaped walls can also differ considerably in comparison to rectangular walls when subjected to lateral loading; for bending about the minor axis which causes the web of the C-shaped wall to go into compression (WiC), the reinforcement in the flanges is likely to yield and this results in substantial plastic deformations. However, when the web of the C-shaped wall is in tension (WiT), a non-ductile and brittle failure can occur due to the large (governing) compression strains (and stresses) needed to balance the tensile forces developed by the web's longitudinal reinforcement. These loading scenarios and idealised strain distributions are illustrated in Figure 1.

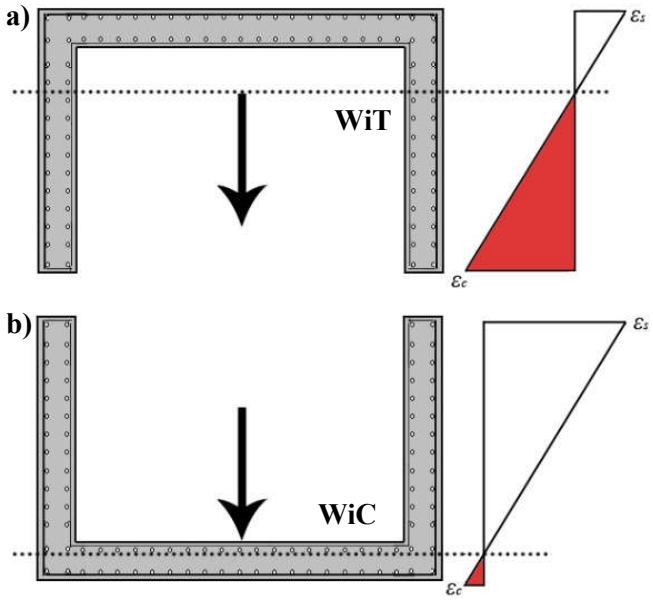

Figure 1 (a) compression governing (WiT) and (b) tension governing (WiC) C-shaped walls

The Pyne Gould building collapsed in a non-ductile, brittle and catastrophic fashion during the February 22nd, 2011 Christchurch earthquake. While it was estimated that the west wall of the Pyne Gould core yielded in vertical tension between levels one and two, Beca (2011) estimate that the east wall failed disastrously in vertical compression. These core walls had no boundary elements or confinement, as this was not a requirement of the design codes at the time of construction. This is also highlighted in CERC (2012), where 'the wall lacked the confining reinforcing needed to provide the ductility required to withstand the extreme

actions that results from the February 2011 aftershock'. Poor performance of non-rectangular RC walls was also observed in major populated centres in Chile following an earthquake in 2010. Wallace *et al.* (2012) particularly emphasised the inadequate behaviour exhibited by poorly detailed and/or compression-controlled RC walls that had insufficient confinement to withstand a 'stable compression zone and ensure spread of plasticity by confining core concrete and supressing rebar buckling'. This is of major concern for non-rectangular RC walls in low-to-moderate seismic regions, which can be: (i) prone to a compression controlled performance (Figure 1), and (ii) lack confinement in the boundary regions of the wall, which is typically not a requirement in the current building codes and Standards (e.g. AS 3600:2009).

Although C-shaped walls are common in the RC building stock of regions of low-to-moderate seismicity, there have been very few studies and experimental tests conducted on non-rectangular RC walls (Beyer *et al.*, 2008a; Constantin & Beyer, 2014). In the limited tests on C-shaped wall sections that have been conducted to date (Beyer *et al.*, 2008b, Constantin & Beyer, 2016, Lowes *et al.*, 2013, Reynouard & Fardis, 2001, Sittipunt & Wood, 1993), the test specimens generally have high longitudinal reinforcement ratios and confined boundary regions. There is yet to be experimental testing on lightly reinforced and unconfined C-shaped walls that represent typical sections found in low-to-moderate seismic regions such as Australia. Beyer (2007) noted that it would be 'interesting to investigate the behaviour of U-shaped [or C-shaped] walls in which such boundary elements are either missing or poorly detailed', as the author believed that 'the boundary elements at the corners were essential for the ductile behaviour of the U-shaped walls'. Moreover, the test results from Constantin (2016) further emphasised the importance of 'proper confinement of the flange ends to ensure the wall displacement ductility'.

Therefore, an investigation on the seismic performance of C-shaped walls with detailing commonly found in low-to-moderate seismic regions is warranted. This paper presents an overview of some of the research results from an extensive number of finite element modelling analyses that were undertaken using VecTor3 (ElMohandes & Vecchio, 2013). The equivalent plastic hinge length and confinement of the boundary regions are discussed. Some recommendations are also given for the next revision of the AS 3600.

2. C-shaped walls for low-to-moderate seismic regions

In total, 144 lightly reinforced and unconfined C-shaped walls with varying parameters have been analysed in VecTor3 for the calculation of the equivalent plastic hinge length and force-displacement relationship. Three different wall sizes have been chosen to represent C-shaped RC cores enclosing elevators for a low-rise (LR), mid-rise (MR) and high-rise (HR) building. The number of storeys of the LR, MR and HR C-shaped walls was chosen to be 3, 6 and 12 respectively, which are within the range given in FEMA (2010) and Maqsood *et al.* (2014). Using an inter-storey height of 3500 mm, the effective height ($H_e \approx 0.7H_n$) is approximately 7.35 m, 14.70 m and 29.40 m for the LR, MR and HR wall respectively. The number of elevator cars required for the different rise of building determines the size of the walls based on the recommendations given in RLB (2014). The LR C-shaped wall was assumed to

enclose two elevator cars (2x500kg, 6 person), while the MR C-shaped wall was assumed to enclose three cars (3x900kg, 12 person) and the HR C-shaped wall was assumed to enclose four cars (4x1150kg, 16 person). The internal dimensions (width x depth, in mm) of the 500kg, 900kg and 1150kg elevator cars are 1000 x 1300, 1400 x 1500 and 1500 x 1800 respectively. Therefore, the resulting lengths of the web (L_{web}) and flange (L_{flange}) that were required for the three different walls are given in Table 1. After some discussions with P. McBean (personal communication, February 26, 2016), a consulting engineer and Joint Managing Director of Wallbridge & Gilbert, 200mm thick walls and a length of 600 mm (approximately 2 ft) for the returns (L_{return}) were taken as values that reflect current and past practice in Australia. The thickness (t_w) of the HR C-shaped wall was increased to 250 mm, as shown in Table 1. Figure 2 illustrates the model in three dimensions for the 3 different C-shaped walls in VecTor3.

Table 1 Dimensions of the C-shaped walls

Wall	t_w (mm)	L_{web} (mm)	L_{flange} (mm)	L_{return} (mm)
LR	200	3600	2000	600
MR	200	6200	2200	600
HR	250	8500	2500	600

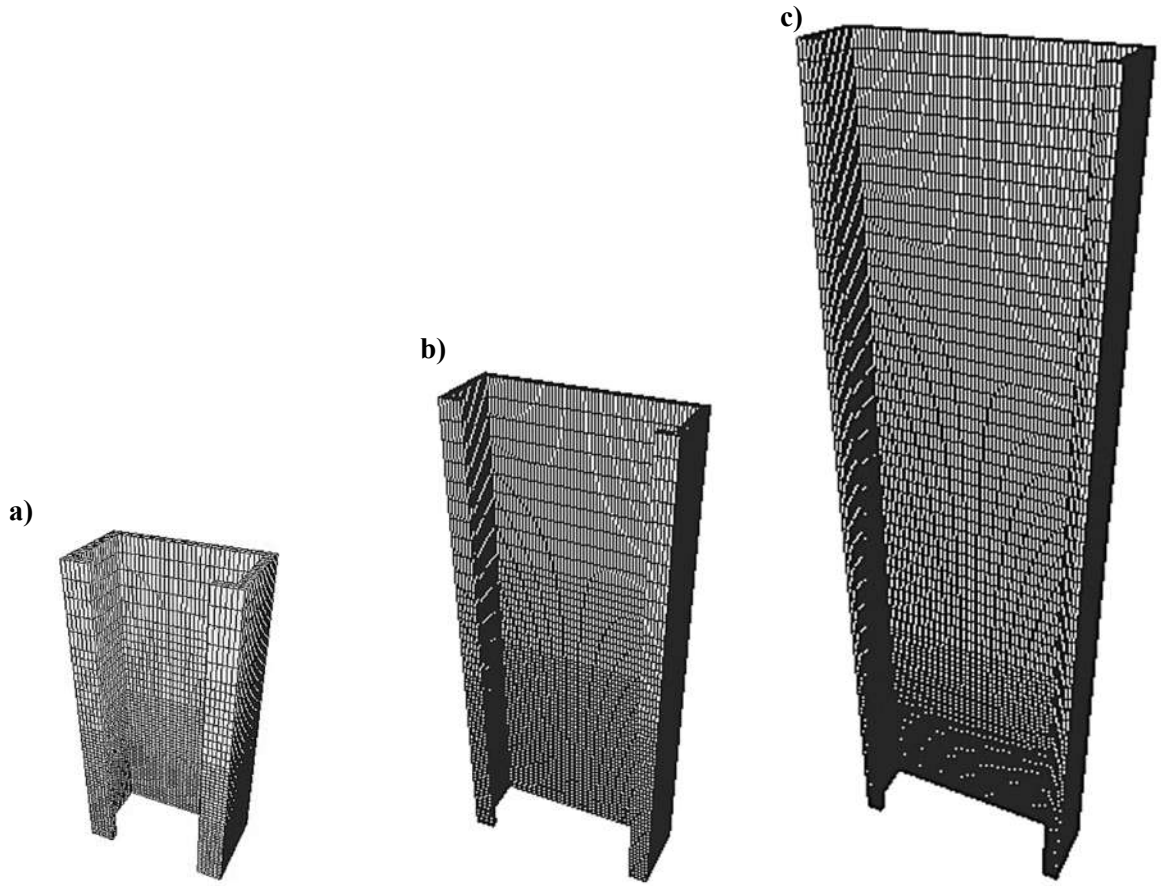

Figure 2 C-shaped walls modelled in VecTor3 for (a) LR (b) MR and (c) HR building (not to scale)

The material and constitutive models that were used in Hoult *et al.* (2017) for VecTor2 were also used in VecTor3 for these C-shaped walls. The range of parameters considered in

VecTor3 are summarised in Table 2. Mean values of the material properties for the reinforcing steel were taken from Menegon *et al.* (2015) for D500N bars, which conform to AS/NZS 4671:2001 (Standards Australia/New Zealand, 2001). The ultimate strain of the reinforcing steel was taken as $0.6\varepsilon_{su}$ based on the recommendations from Priestley *et al.* (2007) when considering potential low cycle fatigue due to cyclic plastic behaviour of the walls.

Table 2 Walls used in VecTor2 with varying parameters

Wall	A_r	H_e (m)	ALR (%)	f_{cmi} (MPa)	ρ_{wv} (%)	ρ_{wh} (%)
LR	2.1[a], 3.7[b]	7.35	1.5, 5	40, 60	0.15, 0.45, 0.70, 1.0	0.25
MR	2.4[a], 6.7[b]	14.70	1.5, 5	40, 60	0.15, 0.45, 0.70, 1.0	0.25
HR	3.4[a], 11.7[b]	29.30	1.5, 5	40, 60	0.15, 0.45, 0.70, 1.0	0.25

a=bending about the major axis
b=bending about the minor axis

The three different directions in which the displacements were applied at the top of the wall corresponded with the wall bending about the major axis and minor axis (with WiC and WiT). Due to time constraints, it was not possible to conduct analyses which involved cyclically varying displacements, so only monotonic behaviour was considered. Failure of the wall was deemed to occur when one of either two things occurred: (i) the Collapse Prevention strain limit was reached in the concrete or steel, for which an unconfined concrete strain value of 0.003 (0.3%), and steel strain value of 0.05 (5%), which is approximately equal to 0.6 times the mean value of ε_{su} given by Menegon *et al.* (2015), were used, or (ii) the maximum displacement was reached corresponding to drift limits of 2.5% for the LR walls and 1.5% for the MR and HR walls. It should be noted that the definition of drift used here corresponds to the displacement at roof level relative to the height of the wall. In VecTor3 it was not possible to control the inter-storey drifts, but simply the overall drift. In AS 1170.4:2007 (Standards Australia, 2007) the inter-storey drift corresponding to the design level earthquake cannot exceed 1.5% of the storey height. It is expected that at average drift levels of 1.5% or 2.5% for these walls, the inter-storey drift requirement from AS 1170.4:2007 will have been exceeded, so that the crack pattern would be reasonably representative of that which could exist at the design level earthquake and there would not be any point in continuing the analyses any further than this.

3. Equivalent plastic hinge length results

For all of the walls analysed in VecTor3, curvature distributions up the height of the wall were obtained by using the concrete and steel strains in the extreme fibre regions at the point at which the maximum displacement was reached. The plastic hinge length (L_p) was calculated using the EPHL method; this method is discussed in more detail in Mortezaei and Ronagh (2012) and Hoult *et al.* (2017). Figure 3 illustrates the equivalent plastic hinge length (L_p) results as a function of the longitudinal reinforcement ratio (ρ_{wv}) for all of the C-shaped walls analysed in VecTor3. It should be noted that for illustrative purposes, the L_p has been normalised to the wall length (L_w) of the C-shaped wall parallel to the direction of

loading in Figure 3. For the C-shaped walls with an insufficient amount of longitudinal reinforcement to allow secondary cracking, a small plastic hinge length can be observed due to the concentration of strains at a single, primary crack. "Single-crack" failure walls typically corresponded to the walls that had a ρ_{wv} less than approximately 0.50% and 0.65%, depending on the f_{cmi} value of the concrete. For the C-shaped walls and bending about the minor axis with web in compression (WiC), a well distributed length of plasticity from the base of the wall is generally achieved as can be observed in Figure 3(b). This is in contrast to the L_p achieved by the C-shaped walls for bending about the major axis (Figure 3a), and about the minor axis with web in tension (WiT) (Figure 3c). For these two modes of bending (and for walls with a sufficient amount of longitudinal reinforcement for secondary cracking), the compression strains govern the performance of the wall; the unconfined compression strain of -0.003 (representing "Collapse Prevention") is reached at low levels of displacement capacity. In many of these walls the steel strains (in the extreme tension fibre) are relatively low when the ultimate concrete strain is reached, which hinders the potential for the plasticity to develop up the wall from the base.

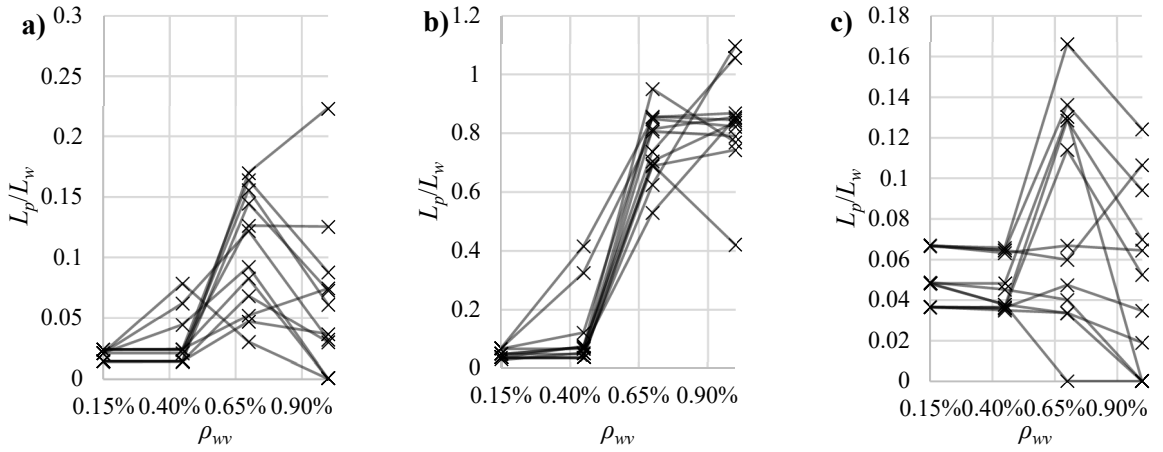

Figure 3 Plastic hinge lengths for the C-shaped walls bending about the (a) major axis (b) minor WiC and (c) minor WiT

Figure 4 gives the longitudinal tension strain distribution estimated from the numerical analysis at a cross-section at the base of a MR wall, and for bending about the major axis, when a displacement of 40 mm is reached at the top of the wall (representing the Collapse Prevention performance level). VecTor3 predicted that the concrete strains were concentrated at the corners of the "boundary regions" (Figure 4b), and not spread out evenly over the width of the web or flange, as is usually assumed in bending theory. This can be understood by the shear lag phenomenon (Kwan, 1996), where the Bernoulli-Euler assumption that plane sections remain plane after bending is only approximate. In reality, a shear flow would develop between the web and flange sections of the wall and there would be a "lag" of the longitudinal displacements in parts of the web (or flange) that are away from the intersection of the two sections (Kwan, 1996). This is illustrated for a C-shaped wall in Figure 5 and bending about the major axis and minor axis (WiT). It should be noted that this has also been observed in the experimental testing from Constantin & Beyer (2016).

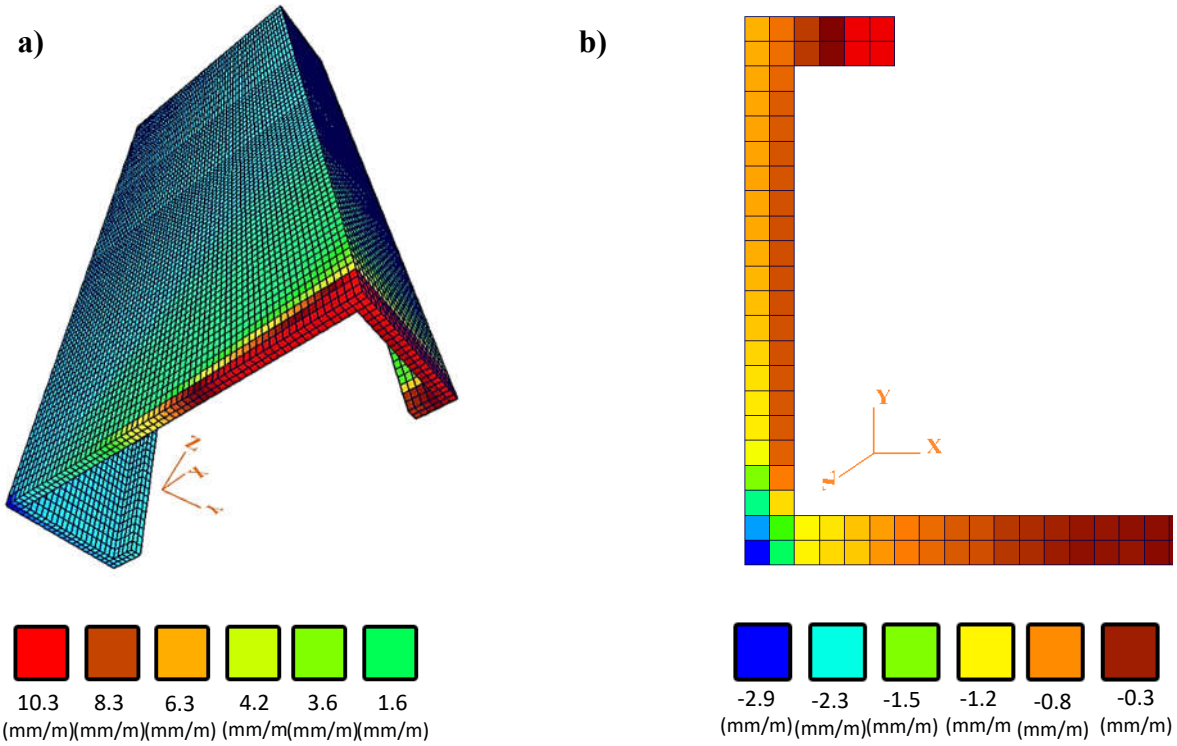

Figure 4 MR wall with strains in (a) tension (steel) (b) compression (concrete) at 40 mm top wall displacement

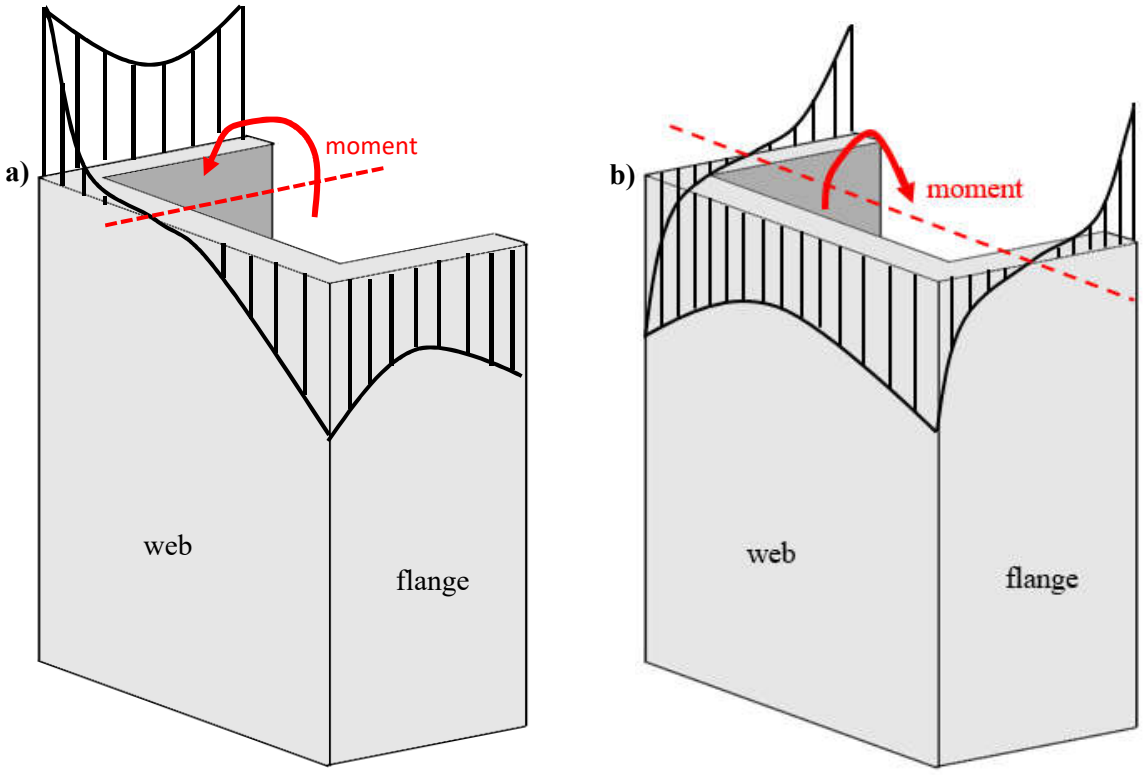

Figure 5 Axial stress distribution in a C-shaped wall due to shear lag for bending about the (a) major axis and (b) minor axis (WiT)

These results will ultimately lead to the derivation of equivalent plastic hinge length (L_p) expressions for lightly reinforced and unconfined C-shaped walls and for the different

directions of loadings. The manuscript with these results and expressions is currently under review for publication.

4. Confinement of the boundary ends

To illustrate the effect of having some confinement provided in the boundary regions of the wall, i.e. those regions at the ends of the flanges and where the web intersects the flanges, further nonlinear pushover analyses were conducted on the MR C-shaped walls with some minor modifications to the models. The transverse reinforcement ratios (ρ_{wh}) in these boundary regions were increased to 1% (in both the x and y directions). This is illustrated in Figure 6 which shows the cross-section of the VecTor3 model of the MR wall and the amount of smeared transverse reinforcement in each area of the wall. Moreover, the transverse reinforcement detailing that would be required for a ρ_{wh} (in the x and y) of approximately 1.00% is shown in Figure 7 for the returns of the MR wall. It should be noted that for this example the assumption is that the diameters of the longitudinal reinforcement (d_{bl}) and transverse reinforcement (d_{bt}) are 12 mm, the spacing (s_t) of all the transverse reinforcement (neglecting the original 0.25% minimum provided by the horizontal reinforcement) is 110 mm and the ρ_{wv} is approximately 1.00%. Only the MR walls with an f_{cmi} of 40 MPa, and with ρ_{wv} values of 0.70% and 1.00% (so that they formed secondary cracks), were analysed with confinement. Loading that caused bending about the major axis and about the minor axis with WiT was considered.

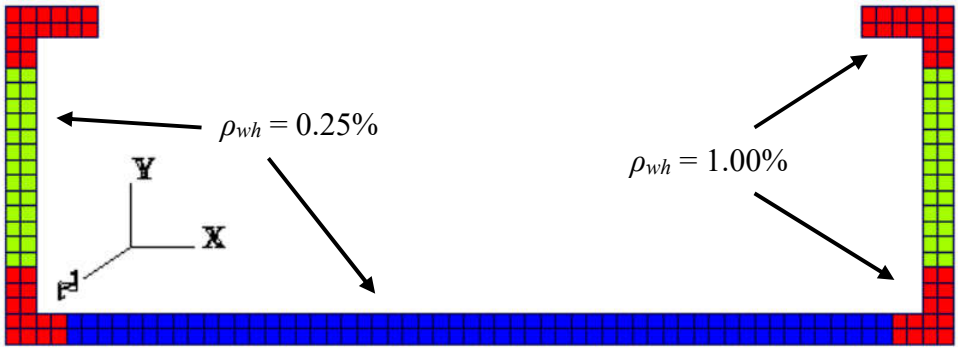

Figure 6 Cross-section of MR C-shaped wall in VecTor3 with confinement

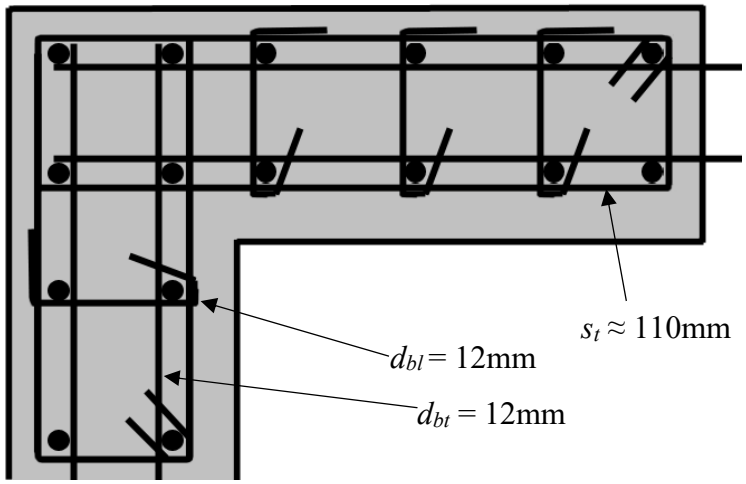

Figure 7 Reinforcement arrangement in the return of the confined MR wall

Figure 8 gives the calculated L_p results for the confined MR walls compared to the same walls without confinement. Similar to the previous section, the L_p has been normalised to L_w in Figure 8. The calculated L_p is observed to be larger for the confined walls in comparison to the length observed for the unconfined walls, in most cases by a factor of approximately 2.

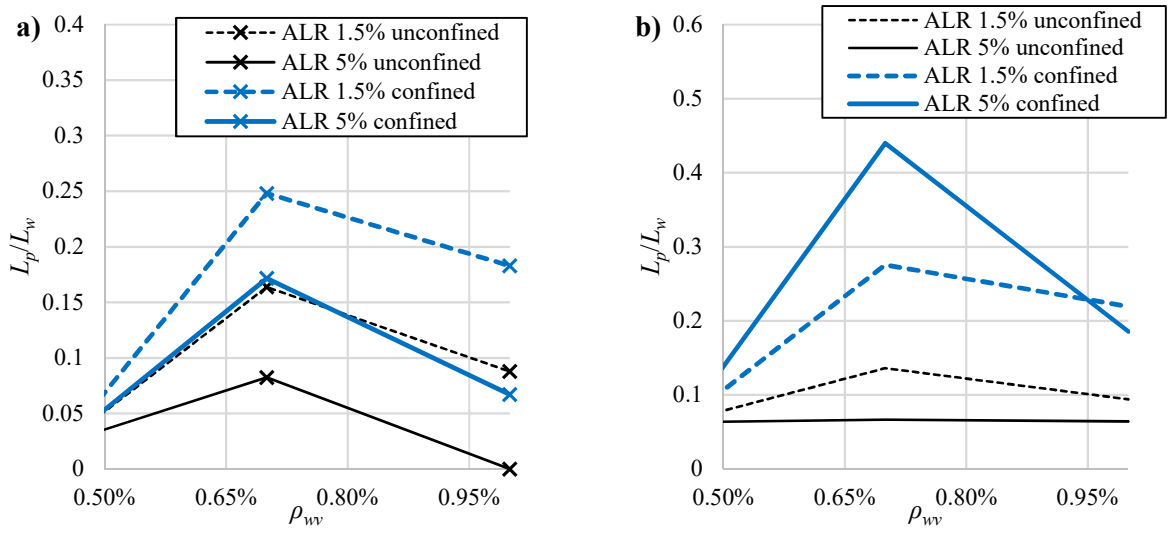

Figure 8 Comparison of L_p for bending about (a) major axis and (b) minor axis (WiT)

The larger calculated equivalent plastic hinge lengths achieved by the confined MR walls, in comparison to the same walls without confinement, also corresponded, of course, to a larger ultimate displacement (Δ_u) capacity being achieved by these walls. An example of this larger displacement capacity is illustrated in Figure 9 for the MR walls analysed with and without confinement for bending about the major axis.

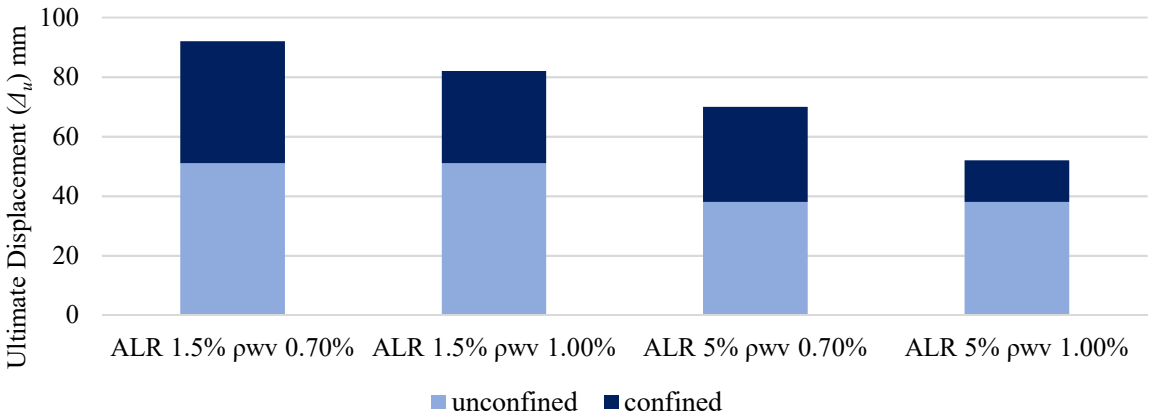

Figure 9 Comparison of the Δ_u achieved by the MR walls bending about the major axis

5. Recommendations for AS 3600 and confinement

One of the proposed additions to the upcoming revision of the Concrete Structures code (AS 3600) is to include a separate section giving the requirements for structures subjected to earthquake actions. Within this section it is specified that boundary elements must be provided in 'limited ductile structural walls' (corresponding to a ductility of 2) in certain situations. According to the proposed revision of AS 3600, which is identical to Section C5.3 in the 2009 version of AS3600:

"In any storey, boundary elements shall be provided at discontinuous edges of structural walls and around openings through them if—

(a) the vertical reinforcement within the storey height is not laterally restrained in accordance with Clause 10.7.4; and

(b) the calculated extreme fibre compressive stress in the wall exceeds $0.15f'_c$.

The stress referred to in Item (b) shall be calculated using the design action effects for the strength limit state, a linear-elastic strength model and the gross cross-section properties of the wall.

Where boundary elements are required, the horizontal cross-section of the wall shall be treated as an I-beam in which the boundary elements are the flanges and the section of wall between them is the web. Restraint of the longitudinal reinforcement in boundary elements shall comply with Clause 10.7.4 of this Standard or, if the extreme fibre compressive stress calculated as above exceeds $0.2f'_c$*, with Clause 14.5.4 of this Standard."*

Part (b) above was originally taken from the ACI 318-95 provisions. This can be traced back to a paper by Wallace and Orakcal (2002). However, Wallace and Orakcal (2002) identified 'significant drawbacks associated with the process'. These 'drawbacks' are explained in detail in Wallace and Orakcal (2002), which include the argument that a stress limit of $0.15f'_c$ is very likely to be exceeded for walls of 'reasonable configured buildings', thus requiring well-detailed boundary regions and over a significant height of the wall. Another

disadvantage is that the stress check, as an index for assessing whether a wall needs detailed boundary elements, is that it cannot distinguish 'between cases where low or high levels of compressive strains are expected' (Wallace & Orakcal, 2002). Therefore, Wallace and Orakcal (2002) recommended a different approach, which was included in the ACI 318-99 provisions (and subsequent revisions). The revised approach requires boundary elements in the wall if the neutral axis (c) is larger than c_{crit}, the calculated value using Equation 1.

$$c_{crit} = 0.5L_w\varepsilon_{cl}/(\delta_u/h_w) \approx \frac{L_w}{600(\delta_u/h_w)} \quad 1$$

where L_w is the wall length, ε_{cl} is the extreme fibre compression strain (which is subsequently taken as 0.003), δ_u is the design displacement and h_w is the height of the entire wall. Some of these parameters are illustrated in Figure 10 for the deflection at the top of a cantilever wall and equivalent single-degree-of-freedom structure.

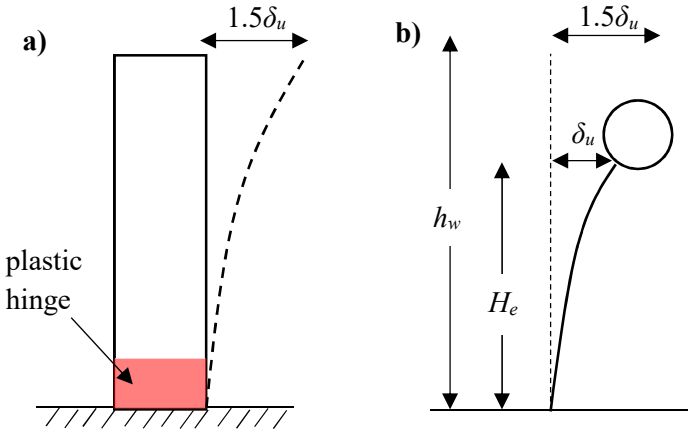

Figure 10 Deflection of (a) cantilever wall and (b) equivalent single-degree-of-freedom structure

This revised approach recommended by Wallace and Orakcal (2002), which is used in the current ACI 318 provisions, is a "displacement-based design" approach; the wall is assumed to displace by rotating about a plastic hinge at the base of the wall and the critical value for the neutral axis depth corresponding to ultimate conditions at the base of the wall is estimated with the equation for c_{crit} (Equation 1). It should be noted that Equation 1 for c_{crit} was revised in ACI 318-14 to account for an earthquake larger than the design level earthquake:

$$c_{crit} = 0.5L_w\varepsilon_{cl}/(1.5\delta_u/h_w) \approx \frac{L_w}{600(1.5\delta_u/h_w)} \quad 2$$

For the purposes of AS 3600 and seismicity in Australia, it would be simpler to assume a certain displacement demand for the 2500-year return period earthquake event. For example, a factor of 2.5 times the maximum displacement demand (RSD_{max}) for the 500-year return period spectra of AS 1170.4:2007 would give a conservative value for the displacement at the effective height of the cantilever wall (and approximately 1.5 times this is needed to find the displacement at the top of the wall). A factor of 2.5 is used, instead of the 1.5 or 1.8 factor that is incorporated in AS 1170.4:2007 and the ABCB (2016), due to the findings of higher

'probability factor' values in low-to-moderate seismic regions in comparison to high seismic regions (Hoult *et al.*, 2015; Leonard *et al.*, 2013; Nordenson & Bell, 2000). It should be noted that the use of RSD_{max} assumes that the building secant period, when the wall is cracked and has yielded, exceeds the "corner period" on the displacement spectra in AS 1170.4:2007 (of 1.5 seconds), and more work is needed to determine whether this holds for low-rise walls in particular. Using the derived spectra in AS 1170.4:2007, with a hazard factor (Z) value of 0.08 (consistent with Melbourne and Sydney), the displacement demand at the top of the wall ($1.5\delta_u$) for the different soil classes is given in Table 3.

Table 3 Displacement demand at the top of the wall for different soil classes

Soil Class	RSD_{max} (mm)	δ_u=2.5xRSD_{max} (mm)	$1.5\delta_u$ (mm)
A_e/B_e	26	66	100
C_e	37	93	140
D_e	59	148	220
E_e	92	230	350

The inherent assumption of the equivalent plastic hinge length (L_p) of $0.5L_w$, which has been incorporated in the derivation of Equation 1 and Equation 2, is an approximate value recommended by many researchers (Paulay, 1986; Priestley & Park, 1984; Wallace & Moehle, 1992). However, this approximate value of L_p (of $0.5L_w$) for walls has primarily been derived from analytical or experimental results for RC walls that are not representative of lightly reinforced concrete walls in regions of low to moderate seismicity. Referring back to the results given in Figure 3 and Figure 8, the resulting L_p is typically much smaller than the $0.5L_w$ recommended by others, which is also consistent with the findings of the L_p for lightly reinforced *rectangular* walls Hoult *et al.* (2017). Therefore, a L_p of $0.2L_w$ is a more reasonable estimate of the L_p for these types of walls (assuming that sufficient detailing has been provided such that secondary cracking can occur and confinement is provided). Taken this into account, Equation 2 can be revised for Australian conditions:

$$c_{crit} = 0.2L_w\varepsilon_{cl}/(1.5\delta_u/h_w) \approx \frac{L_w}{1500(1.5\delta_u/h_w)} \qquad 3$$

where the $1.5\delta_u$ (the displacement demand at the top of the wall) can be (conservatively) taken from Table 3.

It then remains to calculate the length of the wall over which confinement is required and further guidance is given on this within the current ACI-318 provisions.

6. Conclusions

The aim of this paper was to present some preliminary results from an investigation into the seismic performance of lightly reinforced and unconfined C-shaped walls in Australia. As no experimental evidence exists for the performance of such structural elements, a

comprehensive numerical study has been carried out to provide information on the performance of such elements.

The equivalent plastic hinge length (L_p) results were presented for all the C-shaped walls analysed, which were normalised to the wall length (L_w) parallel to the direction of loading. It is important to note that in many of the cases, the unconfined boundary regions of the C-shaped walls were found to play a significant role in inhibiting a good distribution of plasticity on the tension side, even if the wall had a sufficient amount of longitudinal reinforcement to allow secondary cracking. This poor performance was due to the ultimate unconfined concrete strain being reached or exceeded in the extreme compression fibre region at very low displacement capacities. Given that high tensile strains could potentially have been reached in the longitudinal bars on the compressive side due to prior loading in the other direction, the longitudinal bars on the compressive side are likely to buckle as soon as the unconfined concrete crushes, and hence this is a particularly dangerous situation. Further numerical analyses were performed in VecTor3 using the MR walls but with some confinement provided in the boundary regions. The results from the models that included confinement indicated that these walls would have a larger equivalent plastic hinge length, by a factor of about 2 in most cases. Hence the displacement capacity of the walls with confinement also increased substantially. This study has emphasised the importance of confinement in non-rectangular RC walls in order to achieve sufficient displacement capacity to resist rare and very rare earthquakes.

An expression that is used in the ACI 318-14 provisions was altered for Australian purposes, and it is recommended that this be incorporated in the next revision of AS 3600. Equation 3 is a displacement-based design expression which can be used to determine a critical value for the neutral axis depth. If the neutral axis depth is higher than this value then "boundary elements" are needed. It then remains to calculate the length of the wall over which confinement is required and further guidance is given on this within the current ACI-318 provisions. This approach is more appropriate as a design check on the need for boundary elements in RC walls rather than the existing rudimentary stress check.

7. References

ABCB. (2016). The National Construction Code (NCC) 2016 Buildings Code of Australia - Volume One: Australian Building Code Board (ABCB).

Altheeb, A. (2016). *Seismic Drift Capacity of Lightly Reinforced Concrete Shear Walls.* (Doctor of Philosophy), The University of Melbourne.

Beca. (2011). *Investigation into the collapse of the Pyne Gould Corporation Building on 22nd February 2011, Report. 46 pp.* Retrieved from

Belletti, B., Damoni, C., & Gasperi, A. (2013). Modeling approaches suitable for pushover analyses of RC structural wall buildings. *Engineering Structures, 57*, 327-338. doi:http://dx.doi.org/10.1016/j.engstruct.2013.09.023

Beyer, K. (2007). *Seismic design of torsionally eccentric buildings with U-shaped RC Walls.* (PhD), ROSE School. (ROSE-2008/0X)

Beyer, K., Dazio, A., & Priestley, M. J. N. (2008a). Inelastic Wide-Column Models for U-Shaped Reinforced Concrete Walls. *Journal of Earthquake Engineering, 12*(sup1), 1-33. doi:10.1080/13632460801922571

Beyer, K., Dazio, A., & Priestley, M. J. N. (2008b). Quasi-Static Cyclic Tests of Two U-Shaped Reinforced Concrete Walls. *Journal of Earthquake Engineering, 12*(7), 1023-1053. doi:10.1080/13632460802003272

Cardenas, A. E., & Magura, D. D. (1972). Strength of High-Rise Shear Walls - Rectangular Cross Section. *Special Publication, 36*. doi:10.14359/17361

CERC. (2012). Canterbury Earthquakes Royal Commission. Final report: Volume 2: The performance of Christchurch CBD Buildings. Wellington, NZ.

Constantin, R. (2016). *Seismic behaviour and analysis of U-shaped RC walls.* École polytechnique fédérale de Lausanne, Lausanne, Switzerland.

Constantin, R., & Beyer, K. (2014). *Non-rectangular RC walls: A review of experimental investigations*. Paper presented at the 2nd European Conference on Earthquake Engineering and Seismology, Istanbul, Turkey.

Constantin, R., & Beyer, K. (2016). Behaviour of U-shaped RC walls under quasi-static cyclic diagonal loading. *Engineering Structures, 106*, 36-52. doi:http://dx.doi.org/10.1016/j.engstruct.2015.10.018

ElMohandes, F., & Vecchio, F. (2013). Vector3 and FormWorks Plus User Manual. Department of Civil Engineering, University of Toronto. Retrieved from http://www.civ.utoronto.ca/vector/user_manuals/manual6.pdf

FEMA. (2010). HAZUS MH MR5 Technical Manual. Washington, D.C.

Hoult, R., Goldsworthy, H., & Lumantarna, E. (2017). Plastic Hinge Length for Lightly Reinforced Rectangular Concrete Walls. *Journal of Earthquake Engineering*. doi:10.1080/13632469.2017.1286619

Hoult, R. D., Goldsworthy, H. M., & Lumantarna, E. (2015, 1-3 September). *Improvements and difficulties associated with the seismic assessment of infrastructure in Australia.* Paper presented at the Australasian Fire and Emergency Service Authorities Council (AFAC) 2015 conference, Adelaide, South Australia.

Kwan, A. K. H. (1996). Shear Lag in Shear/Core Walls. *Journal of Structural Engineering, 122*(9), 1097-1104. doi:doi:10.1061/(ASCE)0733-9445(1996)122:9(1097)

Leonard, M., Burbidge, D., & Edwards, M. (2013). Atlas of seismic hazard maps of Australia: seismic hazard maps, hazard crurves and hazard spectra *Record 2013/41*: Geoscience Australia: Canberra.

Lowes, L., Lehman, D., Kuchma, D., Mock, A., & Behrouzi, A. (2013). Large-Scale Tests of C-shaped Reinforced Concrete Walls. from NEES Project Warehouse http:///nees.org/warehouse/project/104

Lu, Y., Henry, R. S., Gultom, R., & Ma, Q. T. (2016). Cyclic Testing of Reinforced Concrete Walls with Distributed Minimum Vertical Reinforcement. *Journal of Structural Engineering*, 04016225.

Maqsood, T., Wehner, M., Ryu, H., Edwards, M., Dale, K., & Miller, V. (2014). GAR15 Regional Vulnerability Functions *Record 2014/38*: Geoscience Australia: Canberra.

Menegon, S. J., Tsang, H. H., & Wilson, J. L. (2015). *Overstrength and ductility of limited ductile RC walls: from the design engineers perspective.* Paper presented at the Proceedings of the Tenth Pacific Conference on Earthquake Engineering, Sydney, Australia.

Mortezaei, A., & Ronagh, H. R. (2012). Plastic hinge length of FRP strengthened reinforced concrete columns subjected to both far-fault and near-fault ground motions. *Scientia Iranica, 19*(6), 1365-1378. doi:http://dx.doi.org/10.1016/j.scient.2012.10.010

Nordenson, G. J. P., & Bell, G. R. (2000). Seismic Design Requirements for Regions of Moderate Seismicity. *Earthquake Spectra, 16*(1), 205-225. doi:10.1193/1.1586091

Oesterle, R. G., Fiorato, A. E., Johal, L. S., Carpenter, J. E., Russell, H. G., & Corley, W. G. (1976). *Earthquake Resistant Structural Walls - Tests of Isolated Walls*. Retrieved from Skokie, Illinois:

Paulay, T. (1986). *The Design of reinforced concrete ductile shear walls for earthquake resistance*: University of canterbury, Department of Civil Engineering.

Priestley, M. J. N., Calvi, G. M., & Kowalsky, M. J. (2007). *Displacement-based seismic design of structures / M. J. N. Priestley, Gian Michele Calvi, Mervyn J. Kowalsky*: Pavia : IUSS Press : Fondazione Eucentre, 2007.

Priestley, M. J. N., & Park, R. (1984). Strength and Ductility of Bridge Substructures. National Roads Board, Wellington, New Zealand: RRU Bulletin 71.

Puranam, A., & Pujol, S. (2017, January 9th to 13th). *Minimum Flexural Reinforcement in Reinforced Concrete Walls.* Paper presented at the 16th World Conference on Earthquake Engineering, Santiago, Chile.

Reynouard, J., & Fardis, M. (2001). Shear wall structures. *Cafeel-Ecoest Thematic Report No, 5*.

RLB. (2014). Riders Digest 2014 Adelaide, Australia Edition: Rider Levett Bucknall.

Sittipunt, C., & Wood, S. L. (1993). *Finite element analysis of reinforced concrete shear walls*. Retrieved from

Smyrou, E., Sullivan, T., Priestley, N., & Calvi, M. (2013). Sectional response of T-shaped RC walls. *Bulletin of Earthquake Engineering, 11*(4), 999-1019. doi:http://dx.doi.org/10.1007/s10518-012-9407-2

Standards Australia/New Zealand. (2001). AS/NZS 4671:2001 : Steel Reinforcing Materials.

Wallace, J. W., Massone, L. M., Bonelli, P., Dragovich, J., Lagos, R., Lüders, C., & Moehle, J. (2012). Damage and Implications for Seismic Design of RC Structural Wall Buildings. *Earthquake Spectra, 28*(S1), S281-S299. doi:doi:10.1193/1.4000047

Wallace, J. W., & Moehle, J. P. (1992). Ductility and Detailing Requirements of Bearing Wall Buildings. *Journal of Structural Engineering, 118*(6), 1625-1644.

Wallace, J. W., & Orakcal, K. (2002). ACI 318-99 provisions for seismic design of structural walls. *ACI Structural Journal, 99*(4), 499-508.

Wibowo, A., Wilson, J., Lam, N. T. K., & Gad, E. F. (2013). Seismic performance of lightly reinforced structural walls for design purposes. *Magazine of Concrete Research, 65*, 809-828. Retrieved from

Wilson, J., Wibowo, A., Lam, N. T. K., & Gad, E. F. (2015). Drift behaviour of lightly reinforced concrete columns and structural walls for seismic design applications. *Australian Journal of Structural Engineering, 16*(1), 62-74.